Thermal conductivity from phonon quasiparticles with subminimal mean free path in the MgSiO_{3} perovskite

Dong-Bo Zhang, Philip B. Allen, Tao Sun, and Renata M. Wentzcovitch

Thermal Conductivity from Phonon Quasiparticles with Sub-Minimal Mean Free Path in MgSiO$_3$ Perovskite

Dong-Bo Zhang[1], Philip B. Allen[2], Tao Sun[3], and Renata M. Wentzcovitch[4,5*]

[1]*Beijing Computational Science Research Center, Beijing 100094, China*
[2]*Physics and Astronomy Department, SUNY Stony Brook University, New York 11794-3800, USA*
[3]*Key Laboratory of Computational Geodynamics, University of Chinese Academy of Sciences, Beijing 100049, China*
[4]*Department of Applied Physics and Applied Mathematics, Columbia University, New York, NY 10027, USA and*
[5] *Department of Earth and Environmental Sciences and Lamont-Doherty Earth Observatory, Columbia University, Palisades, NY 10964, USA*

(Dated: August 22, 2017)

Understanding the lattice thermal conductivity at high temperatures is important for many applications. We characterize phonon quasiparticles numerically through a hybrid approach that combines first-principles molecular dynamics and lattice dynamics. We find no lower-bound limits on phonon mean free paths in MgSiO$_3$ perovskite. This contradicts the widely used minimal mean free path idea. The clear identification of phonon quasiparticles validates the use of phonon gas model when phonon mean free paths are shorter than lattice constants of solids. Using the phonon quasiparticle properties, we have calculated the lattice thermal conductivity of MgSiO$_3$ perovskite. The results are reasonable compared to recent experimental measurements.

Compared to electronic and photonic transport, lattice heat conduction is more diverse and less well understood for many materials[1,2]. At high temperature T, thermal conductivity $\kappa(T)$ often has a "saturated" behavior[3–6]. This is an upward deviation from the well-known 1/T scaling[7], suggesting a breakdown of the phonon quasiparticle gas model. The understanding relies on a minimal mean free path (MFP) picture[4,8–11], added phenomenologically to the standard Peierls-Boltzmann phonon gas treatment[12,13]. It is often used for practical investigations[14–16]. In this work, we investigate the phonon gas model and the lattice thermal conductivity (κ_{lat}) of MgSiO$_3$ perovskite (MgPv). We use a recent theoretical advance[17], a hybrid approach that combines first-principles molecular dynamics (MD) and lattice dynamics. MgPv, the most abundant mineral component on Earth's lower mantle, with significant structural complexity, provides an excellent test bed for studying thermal conduction with first-principles calculations. Surprisingly, calculated phonon MFPs do not have the prescribed minima and the computed κ_{lat} agrees reasonably with measured values from ambient pressure (P) to lower mantle P at room temperature and obeys the typical linear dependence on P seen experimentally[18].

The phonon gas model gives the standard understanding of lattice thermal conductivity of crystalline materials[19–21,31]. Peierls-Boltzmann theory describes heat carried by phonon quasiparticles. In relaxation-time approximation (RTA),

$$\kappa_{\text{lat}} = \frac{1}{3}\sum_{q,s} c_{q,s} v_{q,s} \ell_{q,s}, \quad (1)$$

where, $c_{q,s}$, $v_{q,s}$, and $\ell_{q,s}$ are heat capacity, group velocity, and MFP, respectively, for mode (q, s) indexed with wave vector $\mathbf{q}$ and branch s. The MFP is

$$\ell_{q,s} = v_{q,s}\tau_{q,s}, \quad (2)$$

where $\tau_{q,s}$ is the "single mode" phonon relaxation time. This ignores the complication that other modes (q', s') (that couple to mode (q, s)) are also slightly out of equilibrium when

heat flows. The minimal MFP picture[4,9–11] is the belief that a phonon should propagate at least an interatomic distance, or that $\ell_{q,s} > a$, where a is the smallest crystal lattice constant. If not, the minimal MFP idea claims that the phonon picture breaks down and Eq. (1) is no longer valid. The minimal MFP picture hypothesizes a minimum $\kappa_{\text{lat,min}} = \kappa_{\text{lat}}(\ell_{q,s} \to a)$ when MFPs reach their minimal values, $\ell_{q,s} \sim a$. The minimal MFP idea has been regarded as valid phenomenology, useful in various areas from semiconductor physics to mineral physics[14–16].

The fundamental quantity in our hybrid approach[17] is the mode-projected velocity autocorrelation function,

$$\langle V(0)V(t)\rangle_{q,s} = \lim_{t_0 \to \infty} \frac{1}{t_0} \int_0^{t_0} V^*_{q,s}(t')V_{q,s}(t'+t)dt', \quad (3)$$

The normal modes (q, s) have wave vectors $\mathbf{q}$ that are commensurate with the supercell translations $\mathbf{A}_m$, $m = 1, 2, 3$. That is, $\mathbf{q} \cdot \mathbf{A}_m$ is an integer multiple of 2π for all $\mathbf{q}$ and m. The mode-projected velocity for normal mode (q, s) is,

$$V_{q,s}(t) = \sum_{i=1}^{N} \sqrt{M_i}\mathbf{v}_i(t) \cdot \epsilon^i_{q,s} \exp(i\mathbf{q} \cdot \mathbf{R}_i), \quad (4)$$

where, $\mathbf{v}_i(t)(i = 1, ..., N)$ is the atomic velocity produced by first-principles MD simulations using a periodically repeated supercell with N atoms. $\epsilon^i_{q,s}(i = 1, ..., N)$ is the polarization vector of normal mode (q, s) in harmonic approximation, obtained from density functional perturbation theory[32]. M_i and $\mathbf{R}_i$ are the atomic mass and coordinate of atom i in the supercell, respectively. Both M_i and $\epsilon^i_{q,s}$ repeat periodically within the supercell, with the periodicity of the primitive cell.

For a well-defined phonon quasiparticle, the correlator $\langle V(0)V(t)\rangle_{q,s}$ displays oscillatory decaying behavior. It can be characterized by a renormalized phonon frequency, $\widetilde{\omega}_{q,s}$, and a linewidth, $\Gamma_{q,s}$, satisfying the condition $|\triangle\omega_{q,s} - i\Gamma_{q,s}| \ll \omega_{q,s}$, where $\triangle\omega_{q,s} = \widetilde{\omega}_{q,s} - \omega_{q,s}$, with $\omega_{q,s}$ being the harmonic frequency[21,33]. The power spectrum of a well defined phonon

quasiparticle,

$$G_{q,s}(\omega) = \int_0^\infty \langle V(0)V(t)\rangle_{q,s}\exp(i\omega t)dt, \qquad (5)$$

has a Lorentzian-type line shape. The concept of phonon quasiparticles maps the complex anharmonic vibrations onto a non-interacting picture. This enables kinetic gas ($\equiv$ Boltzmann equation) modeling[21].

There is no unique definition of a quasiparticle. They are excitations which do not decay too rapidly. A desirable definition is that some scattering experiment can measure a correlation function with a peaked energy distribution. The measured spectrum should agree with the counting rules of the analog non-interacting system. Phonons in simple insulators, measured with momentum-resolved neutrons, are good examples. Insulators with many atoms N per primitive translational cell have $3N$ harmonic vibrations at each q. This can defeat the ability of neutrons to resolve separate excitations. A computational example is Fig. 1 of our earlier paper[17]. It shows three harmonic normal modes of MgPv, all with the same q, and closely spaced energies $\omega_{q,s}$, blurred into a single spectral peak because of anharmonic broadening. No known experiment can resolve separate peaks and satisfy the $3N$ counting rule. Then we should ask, are there hidden, unmeasureable quasiparticles? Computation indicates yes, because, unlike experiment, it can project onto separate harmonic eigenstates. Further discussion is in the Supplemental Materials.

An important property of quasiparticles is that the time and space evolution of their density distributions N_{qs} is given by a Boltzmann equation. Solution of this equation gives transport coefficients. Two things are missing, and one benefit is added. First, the scattering term in linearized Boltzmann theory is

$$\left(\frac{dN_{q,s}}{dt}\right) = -\frac{N_{q,s} - n_{q,s}}{\tau_{q,s}} - \sum_{q',s'}^{q'\neq q}\Omega_{q,s;q',s'}[N_{q',s'} - n_{q',s'}] \qquad (6)$$

The off-diagonal scattering terms $\Omega_{q,s;q',s'}$ are not available in our approach, forcing the RTA (which usually works well except at low T[34]). Second, the velocity autocorrelation function, when projected onto harmonic basis states, has off-diagonal terms that describe anharmonic mode mixing. These should be computed, and the quasiparticle states should be found by unitary transformation into the basis which has the cleanest diagonal spectrum (least weight in off-diagonal correlations). Fortunately, our investigation of this effect in MgPv indicates that even at T up to 1500K and beyond, such effects are unimportant. The added benefit is higher order anharmonicity. The forces used in our MD computations come from accurate density-functional theory (DFT), with no restriction to lowest order anharmonic forces. The Boltzmann scattering operator is restricted to third order forces[35,36]. But Boltzmann theory uses a formula for the current $\sum \hbar\omega_{q,s}v_{q,s}N_{q,s}$ which lacks anharmonic corrections[31], and our method adopts this also.

To demonstrate the ideas described above, we do Born-Oppenheimer molecular dynamics (BOMD)[37] of MgPv using the LDA and pseudopotentials that have been extensively
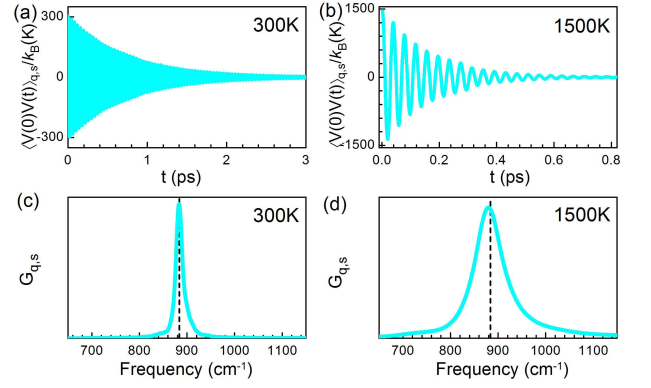

FIG. 1: (a) and (b) show the mode-projected velocity autocorrelation functions of one optical mode (q, s) at $\mathbf{q} = (0, 0, \frac{1}{2})$ obtained at 300 K and 1500 K, respectively, of MgPv with a volume of 24.1 cm³/mol. (c) and (d) show the corresponding power spectra. The vertical dashed lines at 884 cm⁻¹ in (c) and (d) indicate the harmonic frequency of this phonon mode. For (c) and (d), the frequency shifts $\triangle\omega_{\mathbf{q},\mathbf{s}}$ are respectively 2 cm⁻¹ and 10 cm⁻¹, and linewidths $\Gamma_{q,s}$ are respectively 7.3 cm⁻¹ and 34.5 cm⁻¹.

used in previous studies of MgPv[17,38]. Initial atomic structures with *Pbnm* symmetry are first fully relaxed to $P = 0, 10, 40, 80$, and 120 GPa, *via* variable-cell-shape molecular dynamics (VCS-MD)[39]. The resulting volumes V are $24.1, 23.2, 21.3, 19.6$ cm³/mol, respectively. Next, BOMD simulations of $2\times2\times2$ (160 atom) supercells are done at each V for temperatures from 300 to 4000 K, using Nosé-Hoover dynamics[40]. The simulations run for 60 ps with a 1 fs time step, sampling $\mathbf{k} = (0, 0, 0)$ of the supercell Brillouin zone. To improve phase-space sampling, 5 independent runs of 60 ps each are made. In the BOMD simulation, the MgPv crystals are further stabilized by a thermal pressure at high T[41]. The thermal ΔP can be as high as 31 GPa at 4000 K, causing an actual P up to 151 GPa. The wide range of T and P allows systematic study of κ_{lat}. Both BOMD and VCS-MD are implemented with the Quantum Espresso code[42], using the plane wave pseudopotential method[43]. We also do simulations with a $3 \times 3 \times 3$ supercell (540 atoms), and compare the phonon lifetimes with those from the $2 \times 2 \times 2$ supercell (see the Supplementary Material for details[22]). The good agreement indicates that the $2 \times 2 \times 2$ supercell is sufficient to converge the relaxation time $\tau_{q,s}$.

Figs. 1(a,b) show mode-projected velocity autocorrelation functions $\langle V(0)V(t)\rangle_{q,s}$ obtained at T = 300 and 1500 K, of one optical mode at $\mathbf{q} = (0, 0, \frac{1}{2})$ (primitive cell coordinates) for MgPv. The harmonic frequency $\omega_{q,s}$ is 884 cm⁻¹, at $V = 24.1$ cm³/mol. Initial amplitudes $\sim k_{\text{B}}$T indicate equipartition. Because many modes are excited and frequent scattering occurs at high T, $\langle V(0)V(t)\rangle_{q,s}$ decays much faster at 1500 K than at 300 K. More details of the vibrational decay with T are in the power spectra. Figs. 1(c,d) show that both spectra have a single peak, allowing identification of the frequency shift $\triangle\omega_{\mathbf{q},\mathbf{s}}$ and linewidth $\Gamma_{q,s}$. At 300 K (1500 K), $\triangle\omega_{\mathbf{q},\mathbf{s}} \simeq 2$ cm⁻¹ (10 cm⁻¹) and $\Gamma_{q,s} \simeq 7.3$ cm⁻¹ (34.5 cm⁻¹). The criteria for well-defined phonon quasiparticles is satis-

fied for all 480 modes sampled by our MD. The lifetime $\tau_{q,s} \equiv 1/2\Gamma_{q,s}$[31] for this mode is ~ 0.36ps at 300 K, comparable with the experimental values extracted from the infrared spectra[33], and decreases rapidly to ~ 0.07ps at $T = 1500$ K.

Characterization of phonon quasiparticles provides a foundation for investigating vibrational properties using phonon gas theory. The frequency shift $\triangle\omega_{q,s}$ can be used to calculate the anharmonic free energy[17]. Here, the lifetime $\tau_{q,s}$ is used to study the phonon MFP and κ_{lat} within the phonon gas model, given that $\tau_{q,s}$ should hardly differ from the transport relaxation time[34]. Fig. 2 shows that the phonon MFP $|\ell_{q,s}|$, extracted for the mode depicted in Fig. 1, follows the $1/T$ law, as predicted also by the lowest order many-body perturbation theory[21]. This confirms that MgPv is weakly anharmonic [17,44,45]. The small deviation within uncertainty may originate from several factors, such as incomplete phase space sampling in BOMD. What is surprising is, that at $T \sim 500$ K, $|\ell_{q,s}|$ can be shorter than lattice constants, even though this is the fastest of the optical modes at $\mathbf{q} = (0, 0, \frac{1}{2})$, with $v_{q,s} = 3174$m/s. In particular, $|\ell_{q,s}|$ is similar in size to the Mg−O bond length, $\simeq 3.0$Å for MgPv at the volume studied here, when $T > 1200$ K. The MFP $|\ell_{q,s}|$ of all the phonon modes at $T = 1200$ K is shown in Fig. 2(b).

It is worth noting that BOMD, with $2 \times 2 \times 2$ supercells, samples only zone center and high symmetry (primitive cell) zone edge $\mathbf{q}$-points. Therefore, we have carried out a BOMD simulation with a $3 \times 3 \times 3$ supercell at the same volume of 24.1 cm^3/mol at $T = 1200$ K. The larger supercell samples some non-special $\mathbf{q}$-points inside the primitive Brillouin zone. The extracted MFPs summarized in Fig. 2(b) display similar behavior as those extracted from $2 \times 2 \times 2$ supercells. This shows that the size effect of BOMD simulation on phonon lifetime $\tau_{q,s}$ is sufficiently converged (see the Supplementary Material[22] for more detailed comparison between the results obtained with $2\times2\times2$ and $3\times3\times3$ supercells). More importantly, it can be seen that once more, the MFPs are shorter than primitive lattice constants for many modes. Therefore, we argue that this applies for most of the $\mathbf{q}$-points which are not sampled in the current BOMD simulation. Since phonon quasiparticles are well-defined throughout the temperature range of interest, this shows that it is unphysical to assume a lower bound ℓ_{min} comparable to lattice parameters. Therefore Eq. (1) does not suggest that κ_{lat} has a lower limit.

These observations validate the phonon gas model such that calculation of κ_{lat} with Eq. (1) is still physically meaningful even when MFPs are shorter than lattice constants. They also demonstrate the importance of *ab initio* atomistic simulations. Computed $\langle V(0)V(t)\rangle_{q,s}$ depicts the decay dynamics of normal modes due to anharmonic phonon-phonon interactions. Quasiparticles acquire a renormalized frequency $\widetilde{\omega}_{q,s}$, and a linewidth, $\Gamma_{q,s}$ from anharmonic forces. Their accuracy has been verified by reproducing[17] other anharmonic effects, *i.e.* measured thermal shifts for IR active modes. This success enables first-principles calculation of temperature-dependent phonon dispersions and anharmonic free energies. MgPv determines many properties of the Earth's lower mantle. We have previously extracted thermoelasticity[44]. Now we show that our extracted phonon lifetimes enable theoretical predic-
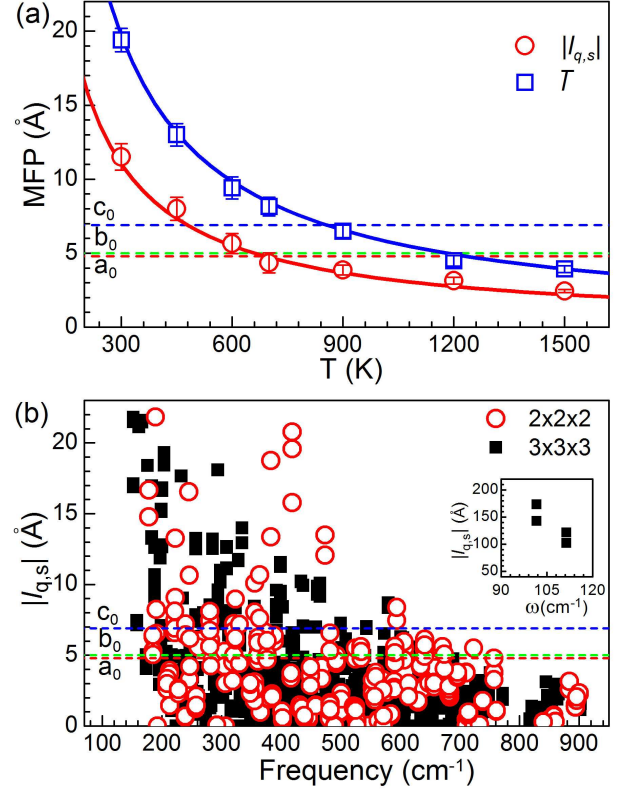

FIG. 2: (a) MFP $|\ell_{q,s}|$ of the mode at $\mathbf{q} = (0, 0, \frac{1}{2})$ with harmonic frequency 884 cm^{-1} (open circles), and averaged MFP $\bar{\ell}$, for all modes at q $= (0, 0, \frac{1}{2})$ (open squares), calculated in the $2 \times 2 \times 2$ MD supercell. Solid curves are $1/T$ fits. (b) MFP $|\ell_{q,s}|$ at 1200 K for all modes with non-zero group velocities calculated in the $2 \times 2 \times 2$ MD supercell (open circles) and in the $3 \times 3 \times 3$ MD supercell (solid squares). The insert shows $|\ell_{q,s}|$ of some acoustic modes at $\mathbf{q} = (0, 0, \pm 1/3)$. In both (a) and (b), the horizontal dashed lines represent the lattice parameters of MgPv, a_0, b_0, and c_0, which define the *Pbnm* primitive cell with a volume of 24.1 cm^3/mol.

tion of κ_{lat} of MgPv. This has important geophysical implications. Heat transport in the mantle is dominated by convection, but conduction plays a role [46]. Conduction is believed to be the main mechanism of heat transport across the core-mantle boundary (CMB) where mass transport is impeded [47]. Thermal conduction properties of the lower mantle are poorly known. Experimental determination of κ_{lat} relies on extrapolation of existing data obtained at low P, T, to high P, T[48]. The reliability of this extrapolation is not yet verified. Recent progress has enabled measurements of κ_{lat} of MgPv to CMB pressures at room temperature[18]. However, available data at ambient conditions do not suffice to give κ at lower mantle conditions.

Fig. 3 shows our calculated κ_{lat} *versus* T and P of MgPv covering the range from ambient to CMB conditions. Relaxation times $\tau_{q,s}$ are found for 60 modes at each sampled $\mathbf{q}$ in our $2 \times 2 \times 2$ supercell BOMD simulations at various T's. We note that BOMD simulations with a similar supercell size have generated satisfactory results for MgO periclase[51]. More dis-
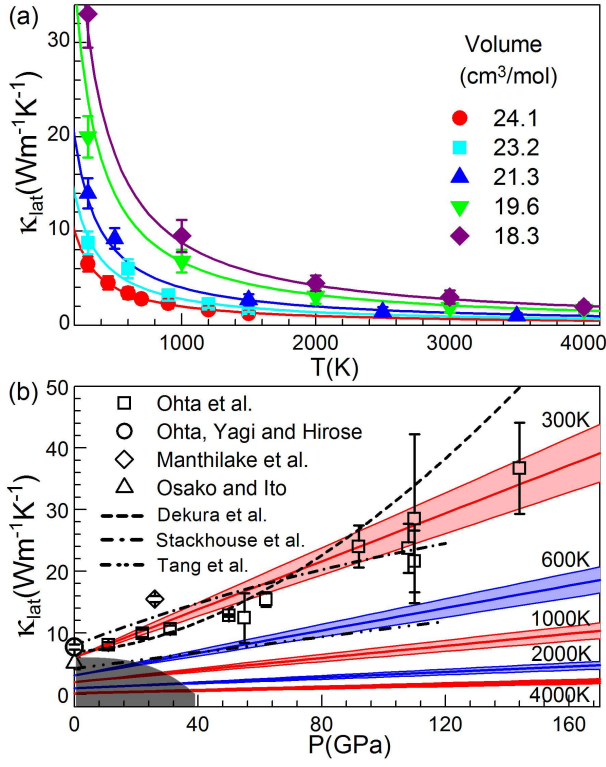
FIG. 3: (a) κ_{lat} *versus* T of MgPv at 5 volumes (solid symbols). Continuous lines show the $1/T$ dependence. (b) κ_{lat} *versus* P of MgPv at 5 temperatures. The shaded areas indicate uncertainties calculated from five parallel BOMD runs. The experimental data (open symbols: □[18], ○[49], ◇[16], △[48]) and theoretical results of other investigators (dashed line[35], dashed dot line[36], and dashed dot dot line[50]) at room temperature are shown for comparison. Error bars are also shown for experimental data. Results under the grey shaded area are not covered in these simulations. They are linear extrapolations to 0 K.

cussion regarding size effect on $\tau_{q,s}$ and κ_{lat} can be found in the Supplemental Material. Phonon velocities $v_{q,s}$ are first calculated from the harmonic phonon dispersion, and then thermal renormalization is added [17]. Availability of thermal renormalization is another advantage of the present approach.

Fig. 3(a) shows that the calculated κ_{lat} follows the typical $1/T$ scaling at constant volume. The small deviations lie within the uncertainties. Results at several volumes allow quantitative characterization of the volume (density) dependence of κ_{lat} in terms of the parameter[52]

$$g = \frac{\partial ln(\kappa_{lat}/\kappa_{lat}^0)}{\partial ln(V_0/V)}, \qquad (7)$$

where κ_{lat}^0 is the value at a reference volume V_0. Calculation of g at $T = 300, 600, 1000, 2000,$ and 4000 K, indicates that g is nearly temperature-independent, with a value of 5.4 ± 0.2. This agrees well with the experimental value $g = 5.6$[18] at 300 K, see Table I.

Since important experimental data were collected at ambient temperature, we have converted $\kappa_{lat}(T, V)$ into $\kappa_{lat}(T, P)$ using a well-established quasiharmonic equation of state[45] obtained using the same techniques employed in this work. Fig. 3(b) shows that the calculated $\kappa_{lat}(T, P)$ agrees well with experimental results from ambient P to lower mantle P at 300 K[18]. The κ_{lat} measured by Manthilake et al.[16] is larger than other experimental reports[18,48] and larger than our prediction (see the Supplementary Material[22] for more analysis). Our $\kappa_{lat}(T, P)$ has a linear P dependence, as also seen in experimental studies of MgPv[18] and MgO[53]. Prediction of κ_{lat} for MgPv by other recent first-principles calculations[35,36,50] are less consistent with experimental data, as shown in Fig. 3(b) and Table I.

To summarize, using the hybrid method combining first-principles molecular dynamics and lattice dynamics, we have studied vibrational properties and calculated κ_{lat} of MgSiO$_3$ perovskite over wide T and P ranges. Investigation of phonon quasiparticles in this system produced unexpected results. Calculated mean free paths are found to have no lower bound limits as prescribed by the minimal mean free path theory. This, together with the well characterized phonon quasiparticles, extends the regime of validity of the phonon gas model. Our finding is based on a thorough analysis of phonon quasiparticles, and is further supported by the agreement of our calculated κ_{lat} with experiments. Our study may shed light on heat transport for a wide range of materials, such as minerals under the extreme conditions of Earth's interior, and semiconductors used for thermoelectric applications.

* Corresponding author; rmw2150@columbia.edu
[1] M. D. Losego and D. G. Cahill, Nature Mater. **12**, 382 (2013).
[2] A. Minnich, J. Phys. Condens. Mat. **27**, 053202 (2015); A.Togo, L. Chaput, and I. Tanaka, Phys. Rev. B **91**, 094306, (2015).
[3] J. F Schatz and G. Simmons, J. Geophys. Res **77**, 6966 (1972).
[4] G. A. Slack, *Solid state physics* vol. 34 (Edited by Ehrenreich, H.,

Seitz, F., and Turnbull, D., Academic, 1979).
[5] A. Auerbach, and P. B. Allen, Phys. Rev. B **29**, 2884 (1984).
[6] D. G. Cahill et al., Appl. Phys. Rev. **1**, 011305 (2014).
[7] M.C. Roufosse and P. G. Klemens, J. Geophys. Res. **79**, 703 (1972).
[8] G. Grimvall, *Thermophysical properties of materials* (Notrh-

TABLE I: Comparison of our calculated parameter g and pressure (P) dependence of κ_{lat} with available first-principles results and experimental measurements.

	This work	First-principles			Experiment	
		Ref.[35]	Ref.[36]	Ref.[50]	Ref.[16]	Ref.[18]
g	5.4 ± 0.2	8.0 ± 0.5	–	–	–	5.6
κ_{lat} vs P	Linear	Nonlinear	Nearly linear	Nearly linear	–	Linear

Holland, 1986).

[9] C. Kittel, Phys. Rev. **75**, 972 (1949).

[10] J. Fabian, and P. B. Allen, Phys. Rev. Lett. **77**, 3839 (1996).

[11] R. Orbach, and A. Jagannathan, J. Phys. Chem. **98**, 7411 (1994).

[12] R. E. Peierls, Ann. Phys. **3**, 1055 (1929).

[13] J. M. Ziman, *Electrons and phonons: the theory of transport phenomena in solids* (Oxford, 2001).

[14] G. A. Slack and P. Andersson, Phys. Rev. B **26**, 1873 (1982).

[15] Y. Chen, A. Chernatynskiy, D. Brown, P. K. Schelling, E. Artacho, and S. R. Phillpot, Phys. Earth Planet. Inter. **210-211**, 75 (2012).

[16] G. M. Manthilake, N. de Koker, D. J. Frost, and C. A. McCammon, Proc. Natl. Acad. Sci. **108**, 17901 (2011).

[17] D.-B. Zhang, T. Sun and R. M. Wentzcovitch, Phys. Rev. Lett. **112**, 058501 (2014).

[18] K. Ohta, T. Yagi, N. Taketoshi, K. Hirose, T. Komabayashi, T. Baba, Y. Ohishi, J. Hernlund, Earth Planet. Sci. Lett. **349-350**, 109 (2012).

[19] A. J. C. Ladd, B. Moran, and W. G. Hoover, Phys. Rev. B **34**, 5058 (1986).

[20] J. E. Turney, E. S. Landry, A. J. H. McGaughey and C. H. Amon, Phys. Rev. B **79**, 064301 (2009).

[21] A. A. Maradudin, and A. E. Fein, Phys. Rev. **128**, 2589 (1962); R. A. Cowley, Adv. Phys. **12**, 421 (1963); T. Sun, X. Shen, and P. B. Allen, Phys. Rev. B **82**, 224304 (2010).

[22] See Supplemental Material at [URL will be inserted by publisher for (i) Size dependence of phonon lifetime; (ii) Sub-minimal mean free paths; (iii) Characterization of phonon quasiparticles with lifetime; (iv) Frequency dependence of lifetime; (v) Lattice thermal conductivity calculated with the minimal mean free path theory and (vi) Anisotropic property of lattice thermal conductivity, which includes Refs.[23–30].

[23] P. G. Klemens, Proc. R. Soc. Lond. A 208, 108 (1951).

[24] C. Herring, Phys. Rev. 95, 954 (1954).

[25] J. Zhou, B. Liao, and G. Chen, Semicond. Sci. Tech. 31, 043001 (2016).

[26] K. Esfarjani, G. Chen, and H. T. Stokes, Phys. Rev. B 84, 085204 (2011).

[27] J. Ma, W. Li, and X. Luo, Phys. Rev. B 90, 035203 (2014).

[28] N. Ghaderi, D.-B. Zhang, H. Zhang, J. Xian, R. M. Wentzcovitch and T. Sun, Sci. Rep. 7, 5417 (2017).

[29] Private communication with K. Ohta (July, 2013).

[30] Private communication with G. M. Manthilake (July, 2013).

[31] T. Sun and P. B. Allen, Phys. Rev. B **82**, 224305 (2010).

[32] S. Baroni, S. de Gironcoli and A. Dal Corso, Rev. Mod. Phys. **73**, 515 (2001).

[33] A. M. Hofmeister, Science **283**, 1699 (1999).

[34] A. J. H. McGaughey and M. Kaviany, Phys. Rev. B **69**, 094303 (2004); A. Ward and D. A. Broido, Phys. Rev. B **81**, 085205 (2010).

[35] H. Dekura, T. Tsuchiya, and J. Tsuchiya, Phys. Rev. Lett. **110**, 025904 (2013).

[36] X. Tang, M. C. Ntam, J. Dong, E. S. G. Rainey, and A. Kavner, Geophys. Res. Lett. **41**, 2746 (2014).

[37] R. M. Wentzcovitch, and J. L. Martins, Solid State Commun. **78**, 831 (1991).

[38] R. M. Wentzcovitch, B. B. Karki, M. Cococcioni, and S. de Gironcoli, Phys. Rev. Lett. **92**, 018501 (2004); R.M. Wentzcovitch, T. Tsuchiya, J. Tsuchiya, Proc. Natl. Acad. Sc. **103**, 543 (2006); K. Umemoto, R. M. Wentzcovitch, and P. B. Allen, Science, **311**, 983 (2006).

[39] R. M. Wentzcovitch, Phys. Rev. B **44**, 2358 (1991).

[40] S. Nosé J. Chem. Phys. **81**, 511 (1984); W. G. Hoover, *Phys. Rev. A* **31**, 1695 (1985).

[41] T. Tsuchiya, J. Tsuchiya, K. Umemoto, and R. M. Wentzcovitch, Earth Planet. Sc. Lett. **224**, 241 (2004).

[42] P. Giannozzi et al., J. Phys. Condens. Matter. **21**, 395502 (2009).

[43] K. Umemoto, R. M. Wentzcovitch, Y. Yu, and R. Requist, Earth Planet. Sci. Lett. **276**, 198 (2008).

[44] R. M. Wentzcovitch, B. B. Karki, M. Cococcioni, and S. de Gironcoli, Phys. Rev. Lett. **92**, 018501 (2004).

[45] B. B. Karki, R. M. Wentzcovitch, S. de Gironcoli, and S. Baroni, Phys. Rev. B **62**, 14750 (2000).

[46] T. Lay, J. Hernlund and B. A. Buffett, Nature Geosci. **1**, 25 (2008).

[47] G. F. Davies, *Dynamic Earth* (Cambridge Univ. Pres. 1999).

[48] M. Osako and E. Ito, Geophys. Res. Lett. **18**, 239 (1991).

[49] K. Ohta, T. Yagi, and K. Hirose, Am. Mineral. **99**, 94 (2014).

[50] S. Stackhouse, L. Stixrude, and B. B.Karki, Earth Planet. Sci. Lett. **427**, 11 (2015).

[51] N. de Koker, Phys. Rev. Lett. **103**, 125902 (2009).

[52] J. M. Brown, Geophys. Res. Lett. **13**, 1509 (1986).

[53] D. A. Dalton, W.-P. Hsieh, G. T. Hohensee, D. G. Cahill and A. F. Goncharov, Scientific Reports **3**, 1 (2013).